

## Supplementary materials

### **Efficient electrochemical oxidation of chloramphenicol by novel reduced TiO<sub>2</sub> nanotube array anodes: kinetics, reaction parameters, degradation pathway and biotoxicity forecast**

Pengqi Wang <sup>a</sup>, Guangyi Chu <sup>b</sup>, Guangfei Gao <sup>a</sup>, Fengchun Li <sup>a</sup>, Yi Ren <sup>a</sup>, Yue Ding<sup>a</sup>,  
Yawei Gu <sup>a</sup>, Wenqiang Jiang <sup>a</sup>, Xuan Zhang <sup>a, 1</sup>

<sup>a</sup> School of Environmental Science and Engineering, Qilu University of Technology  
(Shandong Academy of Sciences), Jinan 250353, China;

<sup>b</sup> Jinan Water & Wastewater Monitoring Center, Jinan 250353, China.

\* Corresponding author.

Prof. Xuan Zhang: zx@qlu.edu.cn

---

<sup>1</sup> \*Corresponding author. Tel: +86-152-691--33848. E-mail: zx@qlu.edu.cn (First)  
Note.

### **List of texts**

**Text S1** CAP conditions were determined by HPLC.

**Text S2** Conditions for detection by HPLC-MS.

**Text S3** Electrochemical test.

**Text S4** Details of various characterization techniques.

**Text S5** Calculation formula for electron transfer rate.

### **List of Figures**

**Fig. S1.** Formation Mechanism of Anodic TiO<sub>2</sub> Nanotubes.

**Fig. S2.** EDS of TNTs.

**Fig. S3.** O 1s XPS spectra of (a) TNTs and (b) R-TNTs.

**Fig. S4.** The kinetic fit curve of CAP degradation using R-TNTs, (a) current density, (b) initial pH and (c) initial concentration on degradation of CAP.

**Fig. S5.** Absolute degradation of different initial pollutant concentrations.

**Fig. S6.** The results of liquid mass spectrometry for degradation intermediates of CAP.

**Supplementary method:****Text S1:** CAP conditions were determined by HPLC

The concentration of CAP in the samples was determined using high performance liquid chromatography (HPLC, LC-20ATvp, Shimadzu, Japan), with the wavelength set at 278 nm. The mobile phase was composed of aqueous solution: methanol = 70:30 (v:v), where the aqueous solution was prepared from 0.005 mol L<sup>-1</sup> sodium heptanesulfonate, 0.05 mol L<sup>-1</sup> KH<sub>2</sub>PO<sub>4</sub>, and 0.5vt% triethylamine. A pH meter (FE20, Mettler Toledo Instrument Co., Ltd.) was employed to determine pH.

**Text S2:** Conditions for detection by HPLC-MS

HPLC-MS (qtof 6550, Agilent, America) was applied to identify the intermediates resulting from CAP degradation. The injection volume (2  $\mu\text{L}$ ), sheath gas flow (12  $\text{L min}^{-1}$ ), sheath gas temperature (350  $^{\circ}\text{C}$ ), column (waters BEH C18) and flow rate (0.3  $\text{mL min}^{-1}$ ) were set, respectively. Formic acid (0.1%) and acetonitrile served as the mobile phases, and the gradient elution settings were 0–2 min, A:B = 5:95, 2–32 min, A:B = 95: 5, and 32–40 min, A:B = 5:95.

**Text S3:** Electrochemical test

A computer-controlled constant potential meter (CHI 760D) was connected to the electrode module. A single-chamber cell with three electrodes was used, consisted of an SCE reference electrode, a working electrode (TNTs or R-TNTs, 1×1 cm) and a Ti plate (1×1 cm) counter electrode. The anode and cathode were separated by a distance of 1 cm and 0.1 M Na<sub>2</sub>SO<sub>4</sub> was chosen as the supporting electrolyte. With a scan rate of 100 mV s<sup>-1</sup>, cyclic voltammetry (CV) was used over a potential range of -1.0 to +2.7 V (*vs.* SCE). Mott-Schottky experiments were performed at an alternate current (AC) level of 10 mV, a potential range of -0.5 to +0.7 V (*vs.* SCE), and a frequency of 1000 Hz.

**Text S4:** Details of various characterization techniques.

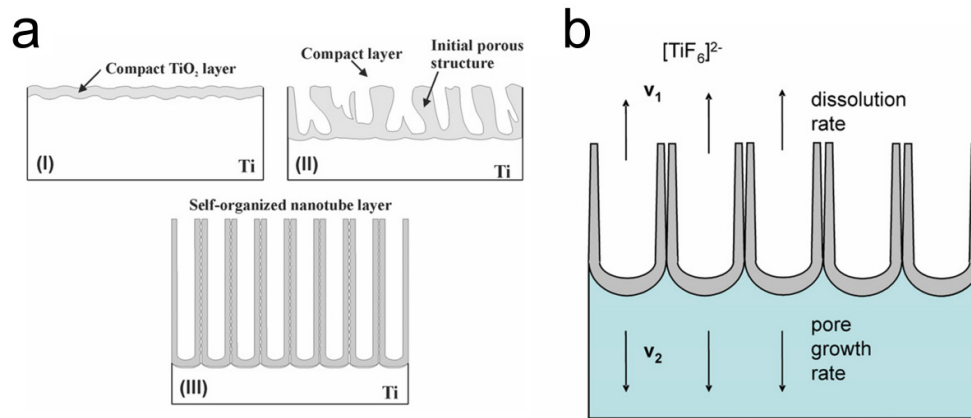
The sample was directly characterized by SEM without gold spraying, and the acceleration voltage was set to 15kv. The X-ray diffraction (XRD) conditions were set as Cu K $\alpha$  radiation and operated at 40kV/40mA. The scanning interval was 10° ~ 85° and the scanning speed was set as 20° min<sup>-1</sup>. The prepared materials were tested using UV-Visible diffuse reflection spectrometer (UH4100, Hitachi, Japan). Integrating sphere component was used, BaSO<sub>4</sub> was used as reference, and the test band was 200-800nm. Raman measurements were performed at room temperature using a Renish modular Raman system with a He-Ne laser 632.8 nm line as the excitation laser, in the range of 100-700 nm.

**Text S5:** Calculation formula for electron transfer rate.

$$\frac{1}{C_{sc}^2} = \left[ \frac{2}{e\epsilon_0\epsilon_N D} \right] \left[ (E_S - E_{fb}) - \frac{kT}{e} \right] \quad (1)$$

where  $C_{sc}$  is the space charge capacitance ( $F/cm^2$ );  $e$  is elementary charge ( $1.602 \times 10^{-19}$  C);  $\epsilon$  is the relative dielectric constant of electrode material (48 for anatase TNTs; assumed to be identical for R-TNTs),  $\epsilon_0$  is the permittivity of vacuum ( $8.85 \times 10^{-12}$  N<sup>-1</sup> C<sup>2</sup>/m<sup>2</sup>);  $E_S$  is the applied potential (V);  $E_{fb}$  is the flat band potential (V);  $k$  is the Boltzmann's constant ( $1.38 \times 10^{-23}$  J/K), and  $T$  is the absolute temperature (K).

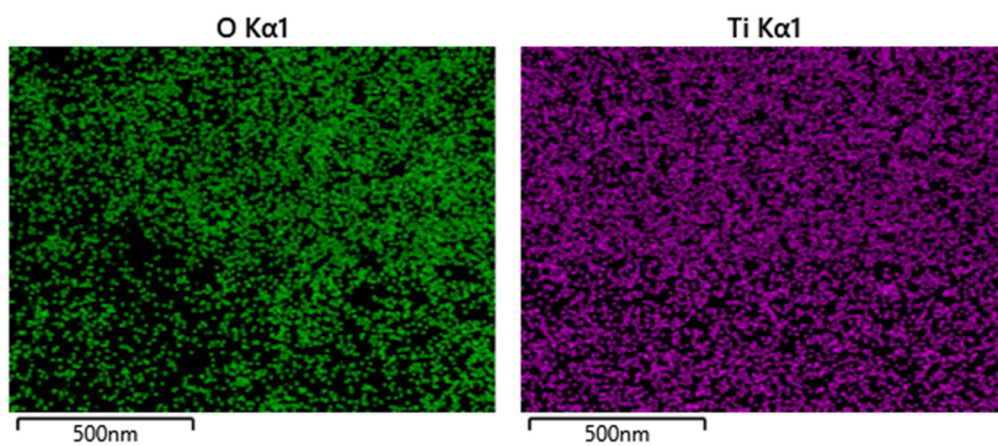
## Supplementary Figures



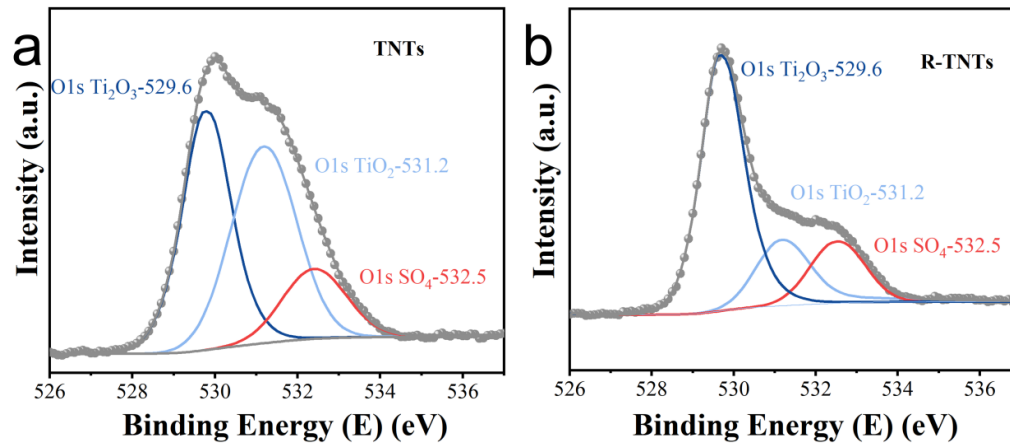
**Figure S1.** (a) The forming process of TiO<sub>2</sub> nanotube arrays. The formation of TiO<sub>2</sub> nanotube arrays can be divided into three different morphological stages (I–III). (I) A barrier oxide is formed. (II) The surface is locally activated and pores start to grow randomly. (III) Self-organized nanotube layer is formed reproduced. (b) steady state growth situation characterized by equal rates of TiO<sub>2</sub> dissolution ( $v_1$ ) and formation ( $v_2$ )[1].

That is in the process of electrochemical anodization, TiO<sub>2</sub> nanotube arrays are formed by self-organization of titania because of three relatively independent procedures: electrochemical oxidation of Ti into TiO<sub>2</sub>, the electrical field-induced dissolution of TiO<sub>2</sub>, and the fluorine ion-induced chemical dissolution of TiO<sub>2</sub>, reaching a delicate balance[1]. Indeed, if the pore initiation phase is followed in a concrete case by SEM images, exactly the sequence described in Fig S1b can be observed[2].

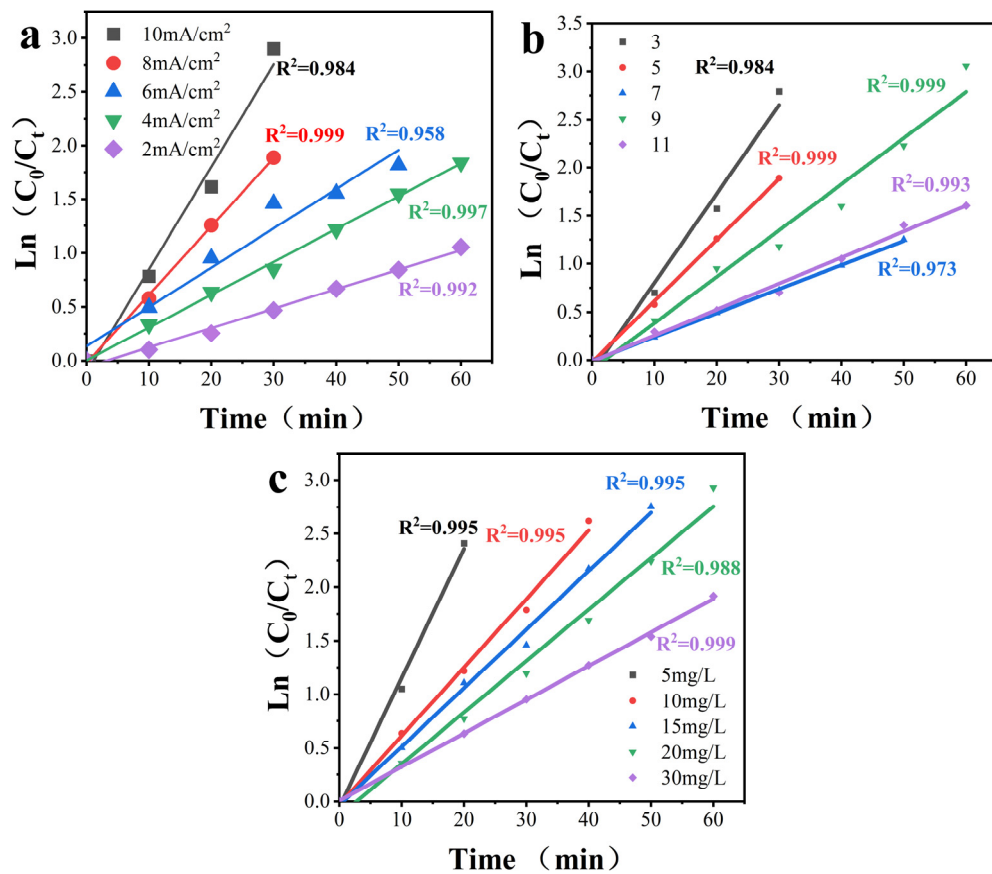
The fact that the layer thickness and the current density reach a limiting value after a certain polarization time can be explained by a steady state situation depicted in Fig S1b[1].



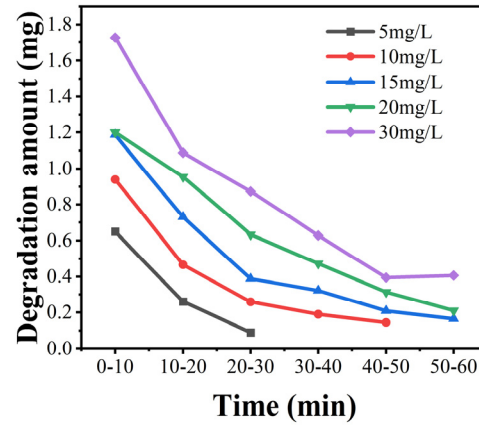
**Figure S2.** EDS of TNTs.



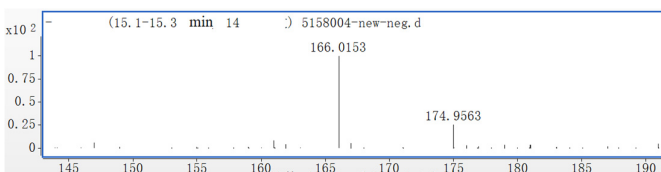
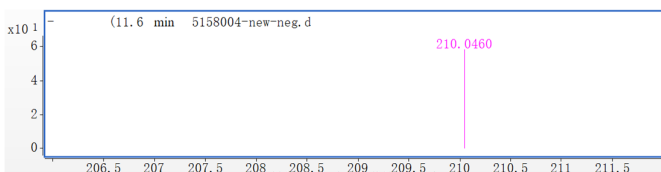
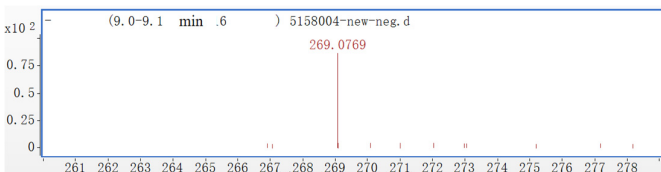
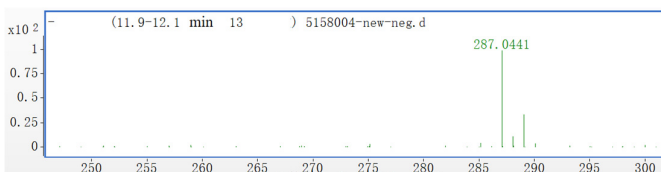
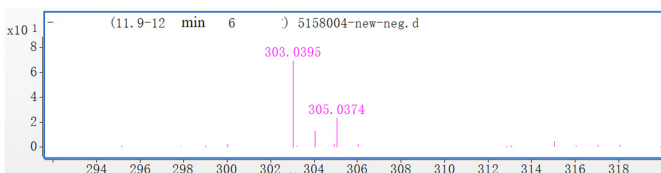
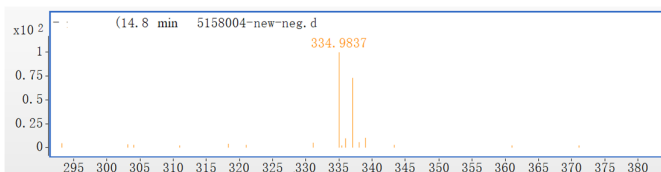
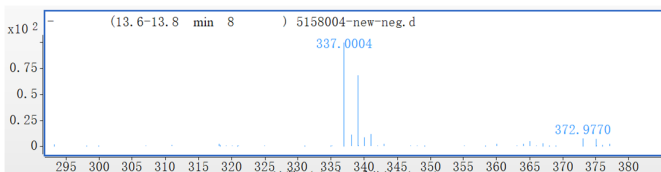
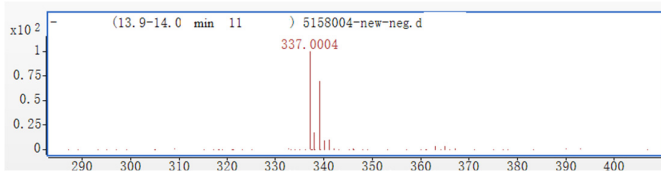
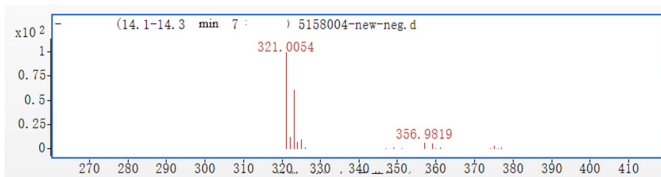
**Figure S3.** O 1s XPS spectra of (a) TNTs and (b) R-TNTs.



**Figure S4.** The kinetic fit curve of CAP degradation, (a) current density, (b) initial pH and (c) initial concentration on degradation of CAP.



**Figure S5.** Absolute degradation of different initial pollutant concentrations.



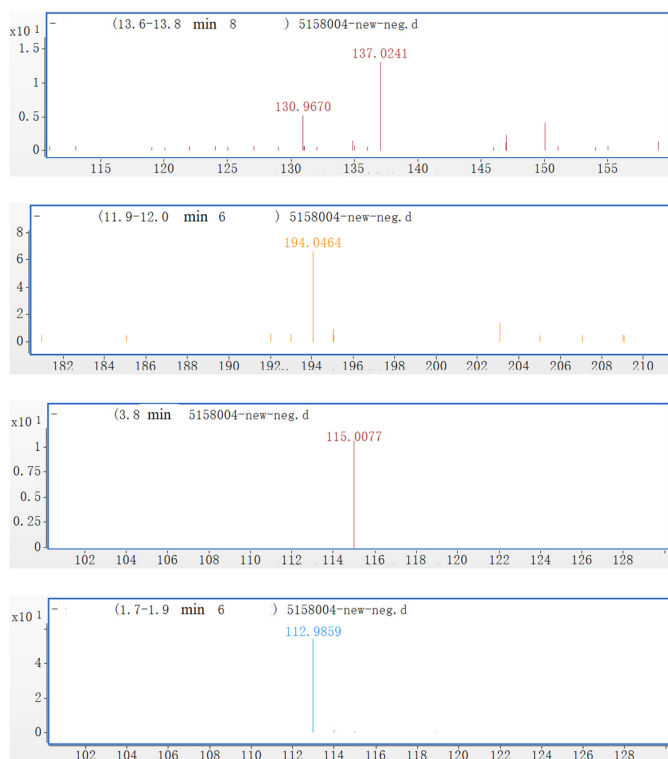


**Figure S6.** The results of liquid mass spectrometry for degradation intermediates of CAP.

1. Macak, J.M.; Tsuchiya, H.; Ghicov, A.; Yasuda, K.; Hahn, R.; Bauer, S.; Schmuki, P. TiO<sub>2</sub> Nanotubes: Self-organized Electrochemical Formation, Properties And Applications. *Curr. Opin. Solid State Mater. Sci.* **2007**, *11*, 3-18, doi:10.1016/j.cossms.2007.08.004.
2. Taveira, L.V.; Macák, J.M.; Tsuchiya, H.; Dick, L.F.P.; Schmuki, P. Initiation and Growth of Self-organized TiO<sub>2</sub> Nanotubes Anodically Formed in NH<sub>4</sub>F / (NH<sub>4</sub>)<sub>2</sub>SO<sub>4</sub> Electrolytes. *J. Electrochem. Soc.* **2005**, *152*, B405, doi:10.1149/1.2008980.